ISSN 0021-3640, JETP Letters, 2022, Vol. 116, No. 10, pp. 698–702. © Pleiades Publishing, Inc., 2022.
Russian Text © The Author(s), 2022, published in Pis'ma v Zhurnal Eksperimental'noi i Teoreticheskoi Fiziki, 2022, Vol. 116, No. 10, pp. 675–680.

CONDENSED MATTER

Self-Sustained Oscillations of the Torque under High-Pressure Torsion in an NdFeB Alloy

A. A. Mazilkin[a, b], S. G. Protasova[a], B. B. Straumal[a, b, c, *], and A. V. Druzhinin[a, c]

[a] *Institute of Solid State Physics, Russian Academy of Sciences, Chernogolovka, Moscow region, 142432 Russia*
[b] *Chernogolovka Scientific Center, Russian Academy of Sciences, Chernogolovka, Moscow region, 142432 Russia*
[c] *National University of Science and Technology MISiS, Moscow, 119049 Russia*
**e-mail: straumal@issp.ac.ru*

Received September 5, 2022; revised September 27, 2022; accepted September 28, 2022

The behavior of an NdFeB-based multicomponent alloy subjected to high-pressure torsion has been studied. The high-pressure torsion results in the partial amorphization of the alloy, where the fractions of the amorphous and crystal phases vary in the process of torsion. The torque increases smoothly with the angle of rotation of anvils, and self-sustained oscillations of the torque appear beginning with a certain torsion (~1000°). The torque varies from 500 to 600 N m with a period of about 1.5 s. The torsion of the alloy in the regime of self-sustained oscillations is accompanied by intense acoustic emission at a frequency of ~1–2 s^{-1}. This phenomenon can be explained by the periodic change in the mechanism of the high-pressure torsion from the dislocation one (characteristic of the crystal phase) to the dislocation-free mechanism (typical of the amorphous state).

DOI: 10.1134/S0021364022602147

Beginning in the mid-1980s, NdFeB-based alloys continue to remain the best materials for permanent magnets [1]. The $Nd_2Fe_{14}B$ compound (T phase [2, 3]) was almost simultaneously synthesized at General Motors Research and Sumitomo Special Metals Laboratories [4]. It demonstrates the record saturation magnetization ($J_S > 1.2$ T) and the record magnetocrystalline anisotropy coefficient ($K_1 > 10^6$ J/m^3) at a fairly high Curie temperature ($T_C > 250$°C). These properties ensure a high stored magnetic energy $BH_{max} > 450$ kJ/m^3 [5]. The coercive force of NdFeB-based alloys is high because ferromagnetic T phase grains are separated from each other by thin nonmagnetic phase layers [6].

The improvement of the properties of materials, including permanent magnets based on the T phase, remains an important aim for the materials science. Such magnets are fabricated from magneto-oriented powders using primarily the liquid-phase sintering method [7] or the melt crystallization method, which allows one to obtain $Nd_2Fe_{14}B$ nanocrystals in the amorphous phase environment [8].

One of the comparatively new methods of the material synthesis is severe plastic deformation [9]. Shear deformation at a high applied pressure can provide a significant melting of samples and is thereby used to synthesize nanocrystalline materials. The application of severe plastic deformation can result in phase transformations [10–14]. Numerous schemes of severe plastic deformation such as high-pressure torsion (HPT), equal channel angular pressing, and helical extrusion have already been developed [15]. Our previous studies of structural changes in NdFeB triple alloys at severe plastic deformation revealed that the HPT can result in their partial [16] or total [17] amorphization depending on the composition. The aim of this work is to study structural changes depending on the strain at the HPT of the NdFeB-based multicomponent alloy used to fabricate permanent magnets.

We examined an NdFeB-based multicomponent alloy close in composition to the alloy studied in our previous work [16]. Atomic emission spectroscopy with inductively coupled plasma showed that the industrial alloy sample had the composition Fe–10.2 Nd–7.6–3.6 Dy–5.5 B–1.2 Co (at %). Disks 0.6 mm thick 10 mm in diameter cut from the sample were subjected to HPT in a Bridgman machine (W. Klement GmbH, Lang, Austria) at room temperature, a pressure of 5 GPa, and an anvil rotation rate of 1 rpm. The machine was PC controlled and made it possible to measure the torque during the torsion. Samples for structural studies were cut from deformed disks at a distance of 2–3 mm from their center. Transmission electron microscopy (TEM) studies were performed on a Titan 80–300 (FEI) microscope at an accelerating voltage of 300 kV. Scanning electron microscopy studies, as well as the fabri-

cation of samples for TEM studies by the focused ion beam method, were carried out on a Versa 3D High-Vac (FEI) microscope. The X-ray diffraction analysis was conducted on a SmartLab (Rigaku) diffractometer (Cu $K\alpha$ radiation).

Figure 1 shows the structure and phase composition of the initial sample subjected to the HPT. X-ray diffraction data (Fig. 1a) indicate that the textured T phase (PDF 2, Entry no. 00-080-0870) and metallic neodymium with the cubic structure (PDF 2, Entry no. 00-089-5330) are present in the samples under study. The scanning electron microscopy image of the structure obtained with a backscattered electron detector (Fig. 1b) clearly demonstrates neodymium-enriched inclusions at triple junctions of grains of the $Nd_2Fe_{14}B$ phase. The neodymium particle size distribution (blue histogram in the right inset) has two maxima at ~1.2 and 5.2 μm. The red histogram in the left inset is the size distribution of $Nd_2Fe_{14}B$ grains with an average size of ~6 μm. The TEM image shown in Fig. 1c also demonstrates the presence of the neodymium-enriched phase region in the form of individual inclusions, as well as the region of triple junctions of T phase grains.

Figure 2a shows the time dependence of the torque during the entire process of deformation. It is seen that the torque increases smoothly with the time and, thereby, with the rotation angle; self-sustained oscillations begin in ~160 s after the beginning of deformation (the rotation angle at this time is about 1000°). The torque varies quasiperiodically from 500 to 600 N m. The deformation of the alloy is accompanied by intense acoustic emission resulting in loud cracks at a frequency of $1-2\ s^{-1}$. Such a behavior under the HPT is atypical of, e.g., the NdFeB ternary alloy [17], where an increase in the torque results in a transition of the system to a steady state. The steady state under the HPT was observed in many materials, in particular, in alloys of copper, aluminum, iron, and titanium [18].

To quantitatively describe self-sustained oscillations of the torque, we used Fourier analysis; the corresponding frequency response is shown in Fig. 2b, where several equidistant maxima are seen. The observed frequency of oscillations of the torque corresponds to a period of ~1.5 s, i.e., almost coincides with the frequency of acoustic emission cracks.

X-ray diffraction spectra of the sample under study are shown in Fig. 3, where only a few rather wide peaks are seen in the region of self-sustained oscillations. The possible presence of the amorphous phase in the structure can be masked by imposition on peaks from crystalline phases. To estimate the degree of crystallinity, we measured the half-width of the main peak in the spectrum ($2\theta = 51°$) of the alloy at various strains (anvil rotation numbers) (see Table 1). It is seen that the half-width of the peak oscillates significantly as a function of the strain rather than varying monotonically.

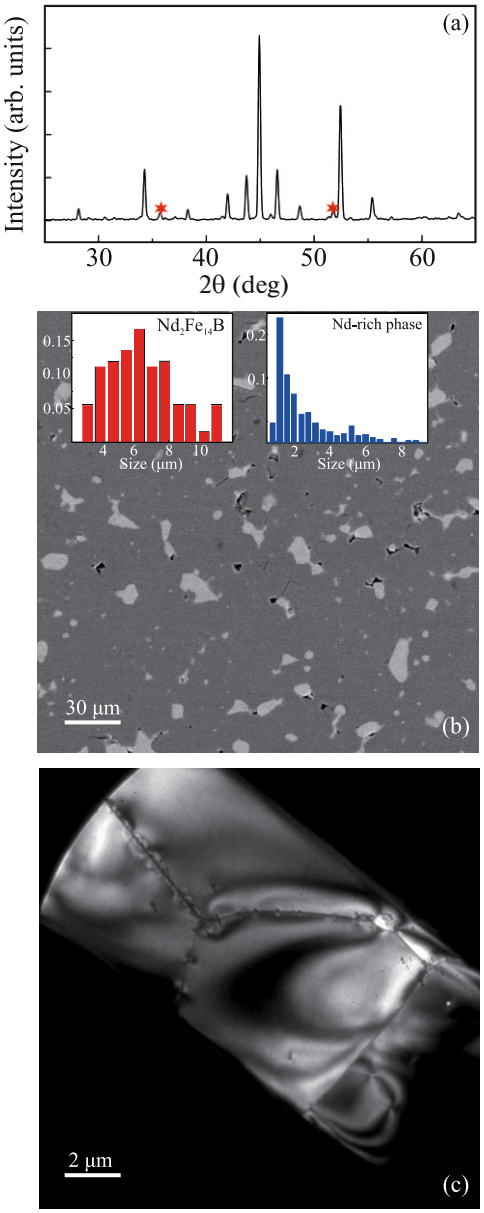

Fig. 1. (Color online) Structure and phase composition of the initial sample of an NdFeB permanent magnet. (a) X-ray spectrum with peaks of the textured T phase (no. 00-080-0870) and of metallic neodymium (no. 00-089-5330); most peaks of neodymium overlap with peaks of the T phase; reflections at $2\theta = 35.68°$ and 51.34° (marked by red asterisks) are seen separately. (b) Scanning electron microscopy image in backscattered electrons; $Nd_2Fe_{14}B$ and neodymium are seen in gray and white, respectively; the insets show the grain size distributions of the corresponding phases for (blue) neodymium and (red) $Nd_2Fe_{14}B$. (c) Transmission electron microscopy image; grains of the T phase with grain boundaries and neodymium particles in triple junctions.

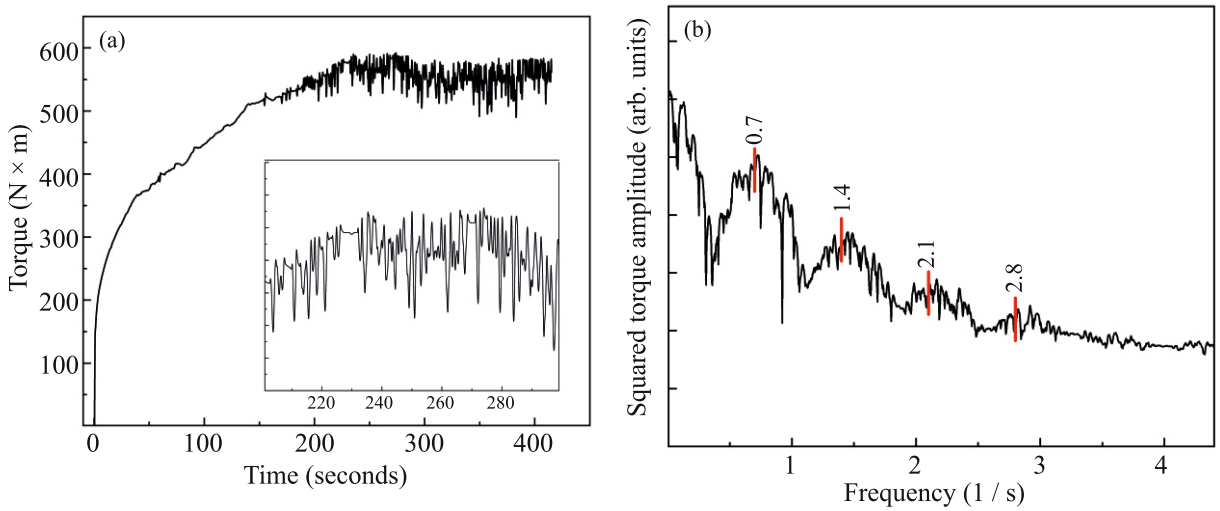

Fig. 2. (Color online) (a) Time dependence of the torque for an NdFeB-based multicomponent alloy at an anvil rotation rate of 1 rpm; the inset shows the scaled horizontal part of the dependence. (b) Frequency response of the torque; dashes with numbers mark the positions of maxima.

Transmission electron microscopy studies show that deformation results in the grinding of the structure. Crystallites of the T phase with sizes of 5 to 15 nm are seen in TEM images of the structure (Figs. 4a and 4b). In addition to the crystalline phase, regions with a contrast characteristic of an amorphous material are also observed in the structure (Fig. 4b). Electron diffraction data also confirm the presence of the amorphous phase. A diffuse halo is seen in the diffraction pattern for the sample with $n = 3.5$ (Fig. 4c). The halo is manifested in the corresponding profiles for $n = 3.5$, 5, and 7 (Fig. 4d) as wide lines with imposed peaks from the crystal part of the structure.

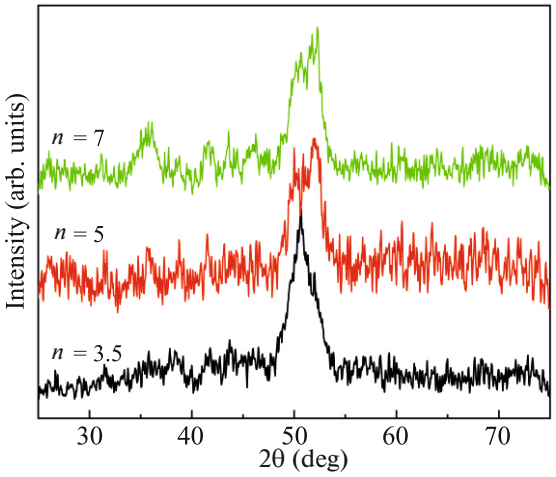

Fig. 3. (Color online) X-ray diffraction spectra of the NdFeB alloy sample deformed by $n = 3.5$, 5, and 7 anvil rotations at an anvil rotation rate of 1 rpm.

Thus, the behavior of the NdFeB multicomponent alloy subjected to deformation significantly differs from the ordinary behavior of materials under similar conditions. It is characterized by self-sustained oscillations of the torque at the middle and later stages of deformation and is accompanied by intense acoustic emission. What is the reason for such a behavior?

It is known that acoustic emission under the deformation of crystalline materials is due to the sharp relaxation of internal stresses, which is caused by the dynamics of dislocation arrays. However, the alloy under study is a mixture of the crystalline and amorphous phases. Mechanisms of deformation in crystalline and amorphous materials are significantly different. Deformation in crystalline materials occurs through the slip or climb of dislocations, as well as through grain boundary sliding. The contribution of grain boundary sliding increases with a decrease in the grain size [19]. The decrease in the grain size in turn complicates the deformation of the lattice through the slip of dislocations because grain boundaries prevent the slip of dislocations from one grain to another according to the Hall–Petch mechanism. At the same time, dislocations are absent in amorphous materials, where any crystal lattice with a long-range order does not exist. Grain boundaries are also absent in them because they are free of regions with differently oriented segments of the crystal lattice. Consequently, amorphous materials are deformed differently, through the formation of sliding strips and motion of their boundaries [20].

If severe plastic deformation is accompanied by the amorphization of the initial crystalline material, mechanisms of deformation change in this process. At the initial stage, when the material is completely crys-

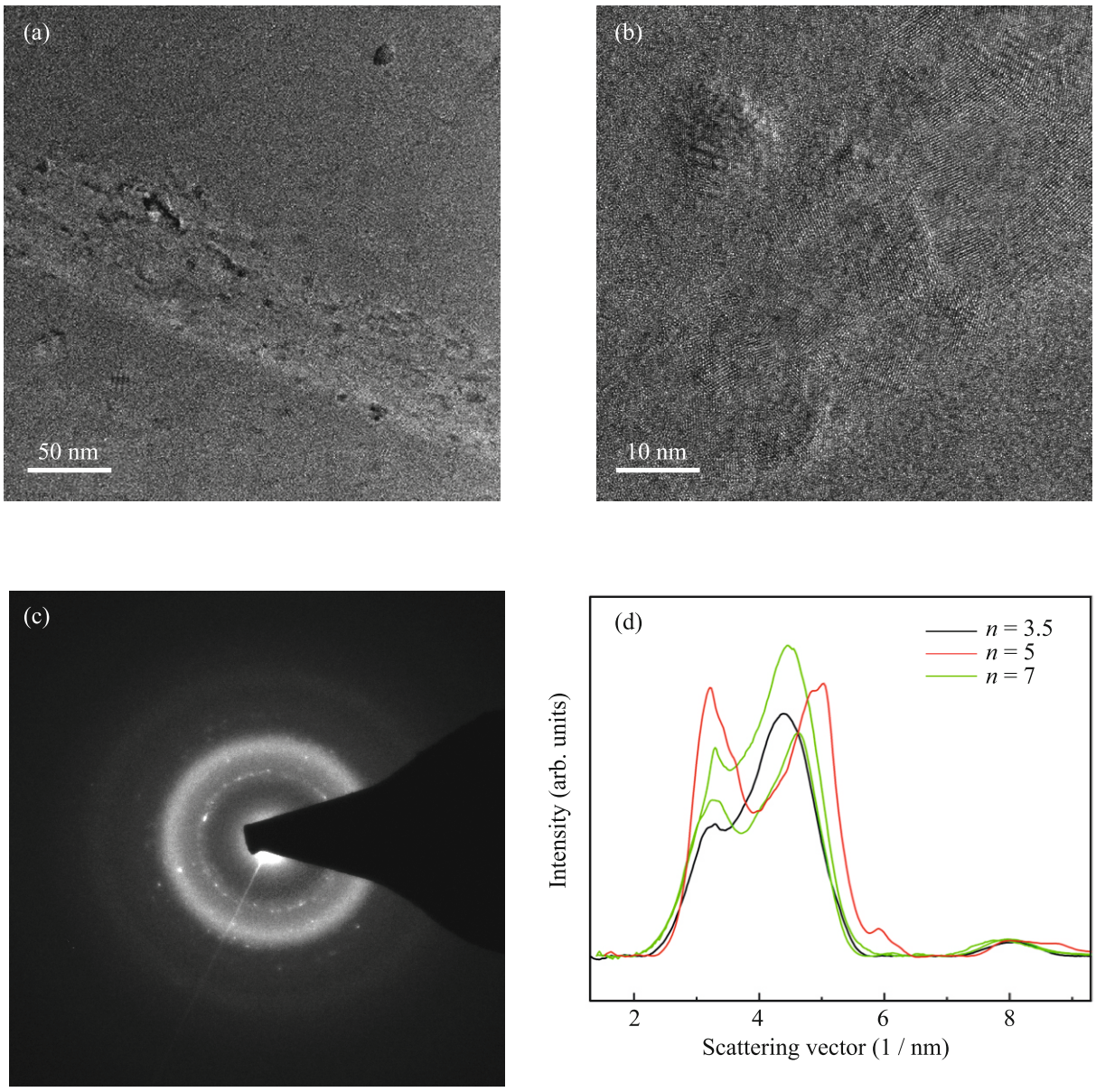

Fig. 4. (Color online) (a, b) Transmission electron microscopy images of the NdFeB alloy in the (a) light-field and (b) high-resolution regime, (c) electron diffraction pattern ($n = 3.5$), and (d) the corresponding radial distribution of the intensity for $n = 3.5$, 5, and 7 anvil rotations.

talline, deformation occurs through the motion of dislocations in the bulk of grains and through grain boundary sliding. Then, as amorphization is developed, the deformation of the amorphous material begins through the formation and growth of sliding strips. The former mechanism almost disappears after the complete amorphization of the entire material.

Table 1. Half-width of a peak in the X-ray diffraction spectrum (see Fig. 3)

Anvil rotation number	FWHM, deg ($2\theta \approx 51°$)
3.5	2.7
5	3.4
7	3.1

It can be assumed that the deformation of the alloy under study is accompanied by a reversible transition of the crystalline to amorphous phase and back. Consequently, the mechanism of deformation and, correspondingly, the velocity and geometry of propagation of sliding strips in the amorphous phase change abruptly. This phenomenon can be responsible for quasiperiodic oscillations of the torque and, correspondingly, acoustic emission. It was already assumed

that severe plastic deformation of amorphous and crystalline phases can be accompanied by a periodic transition of the amorphous to crystalline phase and back. In particular, such a reversible transition was observed in the Ti_2NiCu amorphous–crystalline composite in [21], where the authors showed that the structure of amorphous–crystalline samples subjected to deformation changes in the damping cyclicity mode with the continuous variation of the relation between the amorphous and crystalline components. The authors of [21] explained this behavior by features of the HPT, where the shear strain varies continuously along the radius of the sample at a constant high applied pressure, and believe that the structure of the phase interface plays an important role in this transformation of the amorphous and crystalline phases.

It is remarkable that no acoustic emission was observed from the completely amorphized NdFeB alloy sample after the HPT [17]. In other words, self-sustained oscillations do not occur if only the amorphous phase exists at the steady deformation stage. This additionally supports our hypothesis on the reversible amorphization of the studied alloy subjected to the HPT.

To summarize, we have revealed that the high-pressure torsion of an NdFeB multicomponent commercial alloy results in the formation of a mixed amorphous–crystalline structure, where the fractions of the components vary periodically during deformation. The variation of the phase composition under the high-pressure torsion is accompanied by intense acoustic emission caused by a change in the material deformation mechanism.

ACKNOWLEDGMENTS

The experimental studies were carried out using the equipment of the Joint Use Center, Institute of Solid State Physics, Russian Academy of Sciences. We are grateful to A. Kilmametov (Institute of Nanotechnology, Karlsruhe Institute of Technology, Germany) for assistance in the use of the high-pressure torsion machine and to the Joint Use Center, Institute of Nanotechnology, Karlsruhe Institute of Technology, Germany, for the access to the Titan 80-300 microscope.

FUNDING

This work was supported by the Russian Science Foundation (project no. 22-23-00613).

CONFLICT OF INTEREST

The authors declare that they have no conflicts of interest.

REFERENCES

1. T. Schrefl, J. Fidler, and H. Kronmüller, Phys. Rev. B **49**, 6100 (1994).
2. K. H. J. Buschow, Mater. Sci. Rep. **1**, 1 (1986).
3. M. Sagawa, S. Fujimura, N. Togawa, H. Yamamoto, and Y. Matsuura, J. Appl. Phys. **55**, 2083 (1984).
4. J. Lucas, P. Lucas, T. le Mercier, A. Rollat, and W. Davenport, *Rare Earths: Science, Technology, Production and Use* (Elsevier, Amsterdam, 2015).
5. W. Rodewald, *Handbook of Magnetism and Advanced Magnetic Materials, Rare-Earth Transition-Metal Magnets* (Wiley, Chichester, UK, 2007).
6. D. Goll and H. Kronmuller, Naturwissenschaften **87**, 423 (2000).
7. J. F. Herbst, Rev. Mod. Phys. **63**, 819 (1991).
8. A. Manaf, R. A. Buckley, and H. A. Davies, J. Magn. Magn. Mater. **128**, 302 (1993).
9. K. Edalati, A. Bachmaier, V. Beloshenko, et al., Mater. Res. Lett. **10**, 163 (2022).
10. Y. Ivanisenko, X. Sauvage, A. Mazilkin, A. Kilmametov, J. A. Beach, and B. Straumal, Adv. Eng. Mater. **20**, 1800443 (2018).
11. B. B. Straumal, X. Sauvage, B. Baretzky, A. Mazilkin, and R. Valiev, Scr. Mater. **70**, 59 (2014).
12. Y. Ivanisenko, A. Mazilkin, I. Gallino, S. Riegler, S. Doyle, A. Kilmametov, O. Fabrichnaya, and M. Heilmaier, J. Alloys Compd. **905**, 164201 (2022).
13. B. B. Straumal, A. R. Kilmametov, A. A. Mazilkin, A. S. Gornakova, O. B. Fabrichnaya, M. J. Kriegel, D. Rafaja, M. F. Bulatov, A. N. Nekrasov, and B. Baretzky, JETP Lett. **111**, 568 (2020).
14. B. B. Straumal, A. A. Mazilkin, S. G. Protasova, A. R. Kilmametov, A. V. Druzhinin, and B. Baretzky, JETP Lett. **112**, 37 (2020).
15. R. Z. Valiev, B. Straumal, and T. G. Langdon, Ann. Rev. Mater. Sci. **52**, 357 (2022).
16. B. B. Straumal, A. Kilmametov, A. Mazilkin, S. G. Protasova, K. I. Kolesnikova, P. B. Straumal, and B. Baretzky, Mater. Lett. **145**, 63 (2015).
17. B. B. Straumal, A. A. Mazilkin, S. G. Protasova, D. V. Gunderov, G. A. López, and B. Baretzky, Mater. Lett. **161**, 735 (2015).
18. B. B. Straumal, A. Kilmametov, Y. Ivanisenko, A. Mazilkin, O. Kogtenkova, L. Kurmanaeva, A. Korneva, P. Zięba, and B. Baretzky, Int. J. Mater. Res. **106**, 657 (2015).
19. S. N. Naik and S. M. Walley, J. Mater. Sci. **55**, 2661 (2020).
20. A. L. Greer, Y. Q. Cheng, and E. Ma, Mater. Sci. Eng. R **74**, 71 (2013).
21. R. V. Sundeev, A. V. Shalimova, N. N. Sitnikov, O. P. Chernogorova, A. M. Glezer, Yu. Presnyakov, A. Karateev, A. Pechina, and A. V. Shelyakov, J. Alloys Compd. **845**, 156273 (2020).

Translated by R. Tyapaev